FITNESS, PERFORMANCE AND HEALTH JOURNAL
2025; 4(1): 9-8
Published online 03 26 2025 (https://todoxpublisher.com/index.php/fphj/index)
doi: https://doi.org/10.53797/fphj.v4i1.2.2025
e-ISSN 2821-3785

Investigation of the Impact of m6A-Related Characteristic Genes on Pancreatic Cancer Using Mendelian Randomization and Single-Cell Sequencing

Jie Lin[1.2], Xiaomei Xie[3], Nur Fauwizah Azahar[4], Miaoge Chen[5]， Soon Siew Choo[1*]

[1] MAHSA University, Bandar Saujana Putra, 42610 Selangor, Malaysia
[2]Department of Tumor Radiotherapy, Youjiang Medical College for Nationalities Affiliated Hospital, Baise, Guangxi Province, 533000, China
[3]Youjiang Medical University for Nationalities, Baise, Guangxi Province, 533000, China
[4]MAHSA University, Bandar Saujana Putra, 42610, Jenjarom, Selangor, Malaysia
[5]Department of Gastroenterology, Beiliu People's Hospital, Baise, Guangxi Province, 537400, China

*****Corresponding Author**,** E-mail: siewchoo@mahsa.edu.my

To Cite This Article: Lin, J., Xie, X.., Azahar, N. F.., Chen, M.., & Soon, S. C. (2025). Investigation of the Impact of m6A-Related Characteristic Genes on Pancreatic Cancer Using Mendelian Randomization and Single-Cell Sequencing. *Fitness, Performance and Health Journal*, *4*(1), 9–28. https://doi.org/10.53797/fphj.v4i1.2.2025

Abstract. Pancreatic cancer (PC) is an aggressive malignancy with rapid progression and poor prognosis. The genetic heterogeneity of PC contributes to its malignancy. N6-methyladenosine (m6A) RNA modification and its regulatory factors are associated with poor prognosis and immunotherapy efficacy in PC patients. This study aimed to investigate the impact of m6A-related signature genes (m6ARS) on PC using single-cell RNA sequencing (scRNA-seq) and the Secretion Modification Region (SMR) method with multi-omics data. Methods included AddModule scoring, single-sample gene set enrichment analysis (ssGSEA), and weighted gene co-expression network analysis (WGCNA) to analyze m6ARS at the single-cell and whole transcriptome levels. The SMR method identified pathogenic genes associated with PC among m6ARS. Patients were stratified into high and low-expression groups based on m6ARS expression, revealing survival differences. Performance was evaluated using receiver operating characteristic (ROC) curves and immunohistochemistry (IHC) staining. Functional and pathway analyses, including GSEA and protein-protein interaction (PPI) networks, were conducted. The clinical value of m6ARS was explored through correlation analysis with clinical parameters, single-cell, and spatial transcriptome analyses, as well as immune microenvironment studies. Drug sensitivity analysis assessed m6ARS's potential role in chemotherapy response. Results identified a turquoise module comprising 882 m6ARS genes at both single-cell and bulk transcriptome levels. SMR analysis found 102 proteins associated with PC, with three key m6ARS genes—GCC2, UBE2D3, and TMX1—showing causal relationships with PC. TMX1 was confirmed as a prognostic marker for PC, with upregulation linked to tumor promotion and worse prognosis. Clinical and immune analyses, as well as drug sensitivity assessments, suggest TMX1's potential as a biomarker for PC prognosis and immunotherapy response. This study integrated single cell sequencing and SMR analysis to identify the shared gene TMX1, emphasizing its potential as a robust prognostic biomarker for PC and its response to immunotherapy. Therefore, targeting TMX1-mediated oxidative stress may represent a novel therapeutic strategy for PC and offer new avenues for future drug development.

Keywords: Pancreatic cancer, N6-methyladenosine (m6A), single-cell RNA sequencing, SMR

**Corresponding author: siewchoo@mahsa.edu.my*

1 INTRODUCTION

According to the GLOBOCAN 2020 data provided by the International Agency for Research on Cancer, pancreatic cancer (PC) is recognized as one of the most fatal malignancies, with nearly an equal number of fatalities (466,000 individuals) and incidences (496,000 individuals) (Sung et al., 2021). Approximately 85% of PCs are classified as adenocarcinomas, whereas pancreatic endocrine tumors make up less than 5% of PCs (Wolfgang et al., 2013). In the early stages, PC typically presents subtle or inconspicuous symptoms. By the time the symptoms become specific enough to suggest PC, the disease may already be at an advanced stage (Hou et al., 2020). Despite advancements in medical technology, the limited efficacy of nonsurgical treatment modalities in addressing the challenges posed by PC continues to hinder progress. The prognosis remains exceptionally unfavorable, with a mere 25% one-year survival rate and a five-year overall survival rate (OS) below 5% (Ansari et al., 2015). Existing treatment and diagnostic techniques for PC are inadequate, emphasizing the need for a primary research focus on the development of innovative prognostic biomarkers, enhancement of early detection rates, and identification of new therapeutic targets to improve survival outcomes. N6-methyladenosine (m6A), a chemical modification found in various RNA species, shows promise as a potential biomarker for diverse biological processes associated with cancer (Liu et al., 2018). As the most prevalent RNA modification in eukaryotes, m6A modification influences gene expression regulation and disease progression by modulating various aspects of RNA biology, including RNA stability, nuclear localization, mRNA splicing, miRNA processing, and mRNA translation (Taketo et al., 2018; Oerum et al., 2021). Numerous studies have confirmed an association between m6A modifications and oxidative stress. However, complex and subtle interactions exist between oxidative stress and m6A modifications in the process of tumor occurrence and progression. It should be emphasized that reactive oxygen species (ROS) have the ability to dynamically regulate the expression and activity of m6A regulatory factors, leading to changes in intracellular m6A levels (Hou et al., 2021). Conversely, m6A modification of genes associated with oxidative stress can potentially exert regulatory control over their own expression, thereby modulating the delicate equilibrium between oxidation and antioxidation as well as influencing the initiation and progression of tumorigenesis (Fu & Zhuang, 2020; Wang et al., 2019). Therefore, understanding the underlying mechanism by which oxidative stress and m6A methylation synergistically contribute to cancer development is of paramount significance for the advancement of tumor therapies.

Mendelian randomization (MR) is a robust technique used to investigate the potential causal association between exposure and outcome by leveraging genetic variation as an instrumental variable (IV) (Davey et al., 2014). Compared with conventional statistical approaches employed in association studies, MR effectively addresses confounding and reverse causality issues, making it increasingly popular for investigating causal mechanisms (Thanassoulis & O'Donnell, 2009; Burgess et al., 2015). We have effectively employed an innovative analysis framework known as the MR/SMR method, which integrates cis-expression quantitative trait loci (cis-eQTL) or cis-DNA methylation QTL (cis-mQTL) with GWAS data. This approach has facilitated the identification of genetic expression or DNA methylation sites associated with a wide range of phenotypic pleiotropy or potential causal relationships (Yang et al., 2021).

In this study, we conducted a comprehensive investigation of the characteristics of m6ARS across multiple omics levels. We employed single-cell and WGCNA methodologies to identify m6ARS and integrated PC data for SMR analysis, which robustly confirmed the causal association between m6ARS and PC as the disease-causing gene. Subsequent analysis revealed that TMX1 is

a potent prognostic biomarker with potential implications in the immunotherapy response for PC. Thus, targeting TMX1-mediated oxidative stress may offer an innovative therapeutic strategy for treating PC, thereby providing valuable insights for future drug development. A workflow diagram illustrating our study is shown in Figure 1.

2 METHOD

2.1 Data collection and processing

We obtained the gene expression profiles and relevant clinical data of TCGA-PAAD patients from the UCSC Xena database. Transcripts per million (TPM) values were extracted for subsequent analysis, with genes exhibiting an average expression level below 0.1 excluded. Samples lacking complete or missing clinicalopathological information were excluded from the study. Furthermore, we retrieved a PC single-cell RNA sequencing dataset (GSE212966) from the Gene Expression Omnibus (GEO) and selected six cases for analysis. The PC spatial transcriptome dataset used in our study was sourced from GSM6177618 within the GEO database. To identify m6A-related feature genes (m6ARS), we compiled a list of 26 previously reported m6A-related genes mentioned in the literature (He et al., 2019).

2.2 Collection and processing of single-cell RNA sequence analysis data

We designated six datasets of single-cell RNA sequencing in pancreatic cancer (PC) as PDAC1, PDAC2, PDAC3, PDAC4, PDAC5, and PDAC6. Subsequently, the single-cell sequencing data were analyzed using the 'Seurat' software package (Stuart et al., 2019). Quality control (QC) was conducted by excluding cells with a mitochondrial gene content below 10% and genes expressed within a range of 200-7000 in at least three cells. Subsequently, we identified 2000 highly variable genes for further analysis. To mitigate batch effects across the six samples, we employed the harmony software package. Cell clusters were constructed using the functions FindClusters and FindNeighbors followed by visualization using the t-SNE method. Finally, simple cell annotation was performed using the SingleR package. The activity of a specific gene set in each cell was quantified using the 'AddModuleScore' function of the Seurat package. To analyze differentially expressed genes (DEGs) between the two groups while keeping other parameters at default values, we utilized the 'FindMarkers' function in the Seurat package with the Wilcoxon test ($p.adj<0.05$) for the statistical significance calculation of DEGs. Genes exhibiting differential expressions between high and low m6A score cells were considered to be involved in m6A at the single-cell transcriptome level and subsequently included in WGCNA analysis at the overall transcriptome level.

2.3 Weighted Gene Co-expression Network Analysis (WGCNA)

Differential gene expression analysis was performed between PC tissues and healthy tissues in TCGA using the "limma" and "pheatmap" packages in R Studio software. The applied criteria were $logFCfilter = 2$ and $adj.P.Val.Filter = 0.05$. Additionally, Weighted Gene Co-expression Network Analysis (WGCNA), a systems biology approach capable of uncovering gene correlation patterns across diverse samples, was employed to identify highly co-varying gene sets (Langfelder & Horvath, 2008). In our study, we utilized the R package 'WGCNA' to conduct WGCNA analysis of TCGA-PAAD bulk RNA-seq data. Initially, we determined an optimal soft threshold β that fulfilled the criteria for constructing a scale-free network. Subsequently, we transformed the weighted adjacency matrix into a Topological Overlap Matrix (TOM) and calculated the

dissimilarity (dissTOM). We employed the dynamic tree-cutting method for gene clustering and module identification. The genes obtained from these modules were designated as m6ARS. Similarly, we acquired lists of m6A-related genes for each module and identified the module with the highest correlation with the m6Ascore for further investigation.

2.4 SMR analysis is used to identify PC-related pathogenic genes

The SMR method proposed by Zhu et al. (2016) integrates summary-level data from genome-wide association studies (GWAS) and expression quantitative trait loci (eQTL) studies to identify genes exhibiting pleiotropic associations with complex traits, thereby enhancing the scientific rigor and academic professionalism of this study. This study employed SMR analysis to identify novel pathogenic genes associated with pancreatic cancer (PC) and investigate their potential functional significance. GWAS data for PC (id: bbj-a-140) were obtained from the IEU Open GWAS project. The eQTL data used in this study were derived from the GTEx v.8 dataset. We utilized the heterogeneity in dependent instruments (HEIDI) test to ensure that significant SMR results indeed indicate pleiotropy or causal relationships rather than being influenced by low correlation linkage models (Zhan & Li, 2024). SMR software (version 1.3.1) was employed to perform SMR and HEIDI tests, with a predetermined significance level of $P < 0.05$ for the former analysis. In the context of the HEIDI test, a P value > 0.05 indicates that linkage disequilibrium does not affect the causal relationship between exposure and outcome, thereby characterizing genes lacking heterogeneity as conservative factors. The intersection genes derived from merging the results of SMR analysis with the module exhibiting maximal correlation with M6Ascore are considered both pathogenic genes associated with PC and m6ARS.

2.5 Performance evaluation and clinical pathological correlation of shared gene features

SMR analysis identified three intersecting genes, namely GCC2, UBE2D3, and TMX1, which exhibited the highest correlation with the m6Ascore. These genes were identified as shared pathogenic genes associated with the m6A-related features. TCGA-PAAD transcriptome data were utilized to validate these shared pathogenic genes by conducting differential analysis between the tumor and normal groups. Genes meeting the criteria of $P<0.05$ were selected for further investigation. To explore the relationship between the expression of these shared pathogenic genes and patient prognosis, they were stratified into high and low-expression groups based on median gene expression levels. Kaplan-Meier (KM) curves were generated using "survminer" and "survival" packages to analyze OS in PC patients. The prognostic efficiency of the model was evaluated by generating ROC curves using the timeROC package. Valuable resources such as protein expression profiles, subcellular localization information, and IHC images were obtained from the Human Protein Atlas (HPA) database (Digre & Lindskog, 2021). The IHC staining images of shared pathogenic genes were obtained from the HPA database, providing visual evidence that demonstrates the differential expression and spatial distribution of these genes between PC and normal tissues. Building upon our previous analysis, we selected TMX1 for further investigation to explore its correlation with clinicopathological parameters.

2.6 PPI network analysis and GSEA enrichment analysis of TMX1 pathogenic gene

We utilized the GeneMANIA database to investigate the interactions between hub genes and their associated genes to gain a more comprehensive understanding of the biological mechanisms and functions in which these genes are implicated. Gene Set Enrichment Analysis (GSEA) is an ontology-based approach that calculates enrichment scores for gene sets and identifies distinct

functional phenotypes (Joly et al., 2021) according to the median level of gene expression. GSEA was used to compare biological pathways between the two groups. The c2.cp.kegg.Hs.symbols.gmt gene set was obtained as a reference from the Kyoto Encyclopedia of Genes and Genomes (KEGG) with a false discovery rate (FDR) < 0.05.

2.7 Analysis of scRNA-seq and stRNA-seq data reveals the expression profile of TMX1 in PC

To investigate the role of TMX1 in the tumor microenvironment (TME) at the single-cell transcriptome level, we examined the expression patterns of TMX1 across various cell types. We used Seurat (version 4.2.0) to analyze stRNA data and assess the expression levels of TMX1 in PC. Spatial spots containing fewer than 300 genes or more than 30% mitochondrial genes were excluded from subsequent analysis. The original counts were normalized using Seurat's transform function, and spatial parameters were determined. Dimensionality reduction was achieved by implementing RunPCA and RunUMAP functions.

2.8 Immune Landscape Assessment

The R package 'GSVA' is used to evaluate the tumor immune microenvironment (TIME) through the ssGSEA method. ssGSEA is an extension of GSEA that can calculate individual enrichment scores (ES) for each sample (Xiao et al., 2020).

The Gene Set Variation Analysis (GSVA) algorithm transforms a gene expression matrix containing individual genes into an expression matrix consisting of specific gene sets and subsequently calculates their enrichment scores (ES) (Hänzelmann et al., 2013). The levels of 16 immune cells and 13 immune-related functions were compared between the high and low-expression groups of TMX1 using ssGSEA scoring. Spearman's correlation analysis was used to investigate the association between TMX1 expression and immune cell infiltration.

2.9 Drug sensitivity analysis

Sensitivity scores for each small-molecule compound in both high-risk and low-risk patient groups were calculated using the pRRophetic package in R software. Subsequently, we used the PubChem website to visualize the 3D drug conformations.

3 RESULTS

3.1 M6A correlation characteristics in single-cell transcriptome

We obtained scRNA-seq data from six patients diagnosed with PC. To mitigate batch effects, we successfully integrated the data from all six samples using the Harmony software package (Figure 1B, C, and D). Subsequently, we performed principal component analysis (PCA) and T-distribution Random neighborhood embedding (t-SNE) to reduce the dimensionality reduction of the first 2000 variants. Clustering was then conducted by identifying the inflection point on the screen plot at 18 (Figure.1E), resulting in a total of 18 clusters with a resolution of 0.2 (Figure.1A). By utilizing marker genes specific to different cell types, we accurately annotated these cells into nine major clusters: memory B cells, bone marrow mesenchymal stem cell-derived chondrocytes, endothelial cells, epithelial cells, macrophages, osteoblasts, multiple CD4+ T cell effector memory subsets, CD8+ central memory T cells, and stem cell types (Figure.1F). To effectively and comprehensively quantify m6A activity across different cell types, we employed the "AddModuleScore" function within the Seurat package to calculate the expression levels of

twenty-six gene sets associated with m6A in all individual cells analyzed (Figure. 1G). Among the nine identified cell types, significantly elevated m6A activity was specifically observed in macrophages， T-cells, and monocytes (Figure.H). Based on m6A activity levels, we further categorized these cells into high or low m6A groups, which allowed us to identify a total of three thousand three hundred two differential expressed genes (DEGs) between these two groups for subsequent analysis.

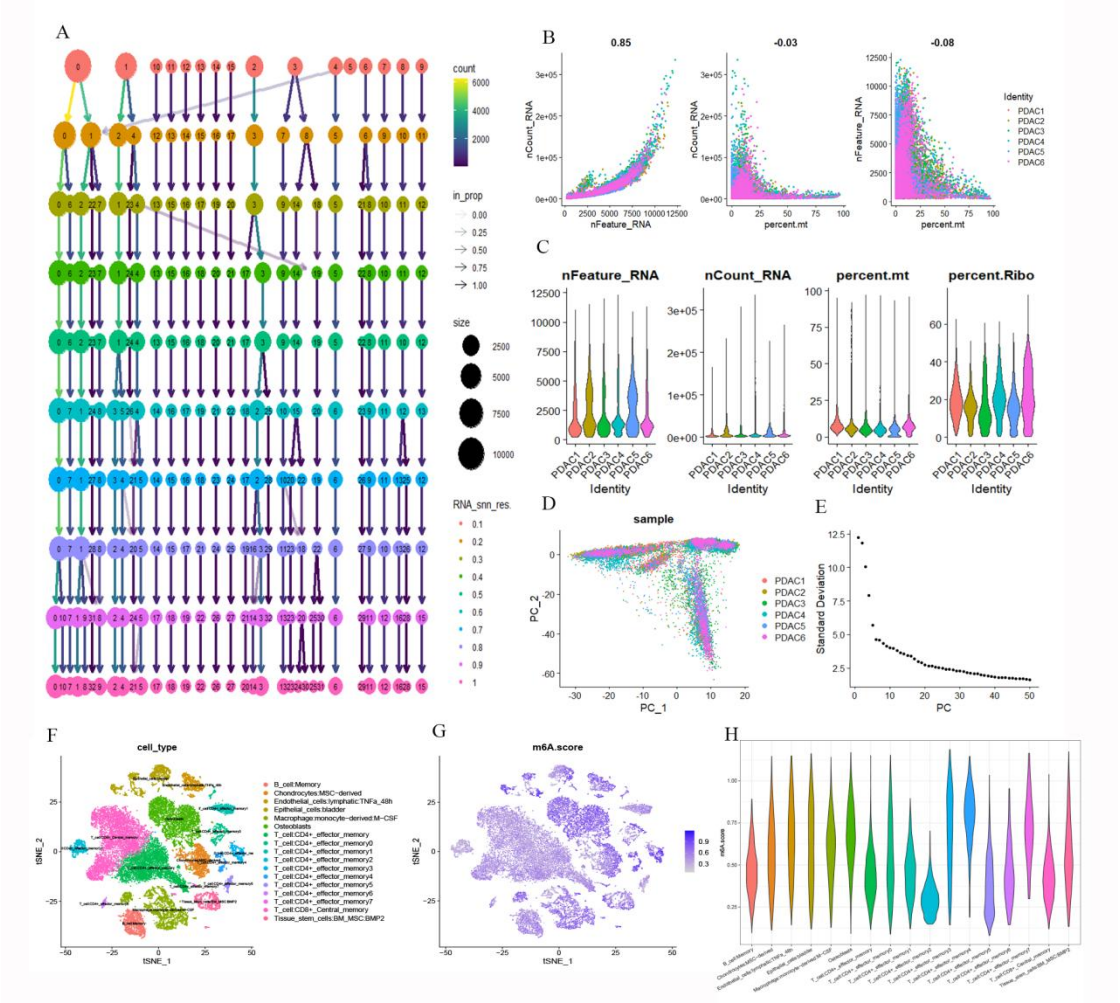

Figure 1 Features of m6A correlation in single-cell transcriptome analysis. **A**. The single-cell transcriptome lineage map illustrates the spatial distribution and relative abundance of distinct cell subpopulations. **B.** analysis of the correlation between RNA features and the ratio of mitochondrial genes to ribosomal genes was performed. **C.** The distribution of RNA features (nFeature_RNA, nCount_RNA, percent.mt, percent.Ribo) in each sample was examined. **D.** PCA analysis elucidates the cellular distribution across different samples while mitigating batch effects. **E.** Heatmap visualization was employed for data representation. **F.** t-SNE plot unveils cell types identified by marker genes. **G.** Activity scoring for m6A in each cell (m6A.score) was conducted. **H.** Distribution analysis of m6A.score among different cell types was carried out.

3.2 Identification of hub modules and M6A-related genes in bulk RNA sequences data

The ssGSEA algorithm is commonly used to assess changes in biological processes and pathway activity of individual samples. In this study, we employed the ssGSEA algorithm to calculate m6A activity scores for each TCGA-PAAD sample as phenotypic data for subsequent WGCNA analysis. To identify modules significantly associated with m6A scores, we conducted WGCNA analysis on the TCGA-PAAD dataset, specifically utilizing 3302 m6A-related outlier-excluded DEGs identified at the single-cell sequencing level to construct a co-expression network (Figure 2.A B). A soft threshold of power= 7 (R2= 0.874) was selected to ensure the establishment of a scale-free topological network in our study. By setting the minimum module gene count to 60 and MEDissThres to 0.25, we successfully obtained six modules (Figure 2.C). Our findings demonstrated that the turquoise module exhibited a robust positive correlation with the overall m6A score in RNA-seq data (cor=0.51), whereas the green module displayed a strong negative correlation with the overall m6A score in RNA-seq data (cor= -0.47, Figure2.D). Furthermore, scatter plots depicting Gene Significance (GS) versus Module Membership (MM) for genes within the turquoise module revealed a significant correlation (cor=0.51, p=3.8e−19, Figure2.E), suggesting the functional relevance of genes within this module to m6A regulation. Therefore, we selected 882 genes from the turquoise module for further analysis (Supplementary Table 1).

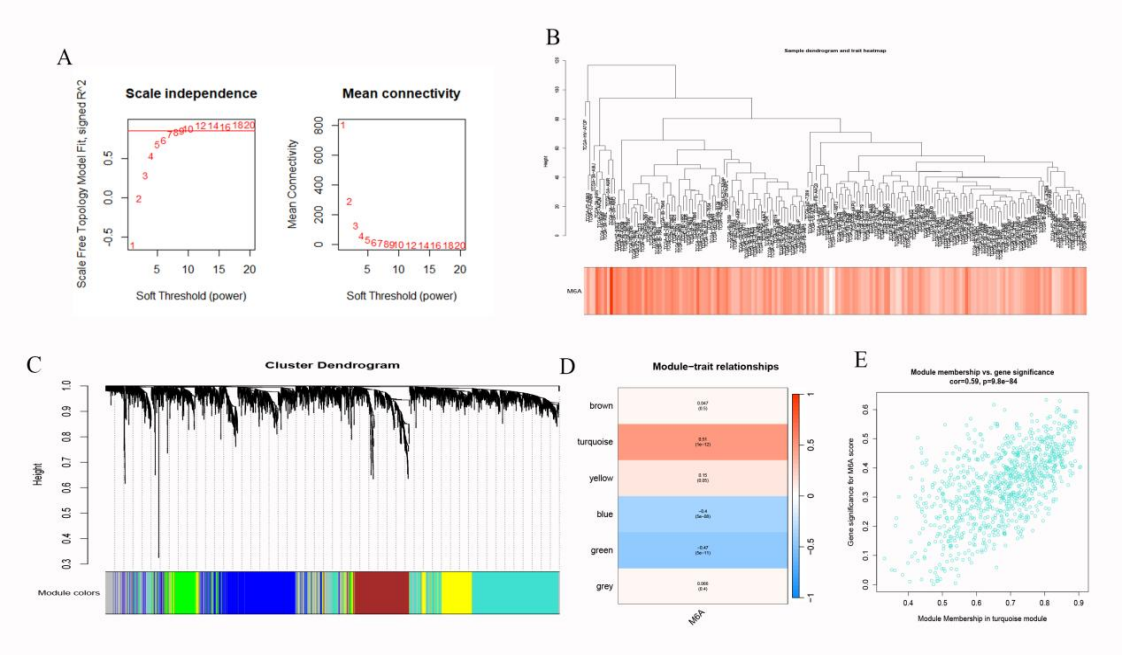

Figure 2 WGCNA analysis. **A.** Soft threshold selection. **B.** The tree graph shows the hierarchical clustering of GEO samples. The heat map at the bottom represents the M6A score for each sample, calculated by the ssGSEA algorithm. **C.** The cluster tree of WGCNA analysis. **D.** Modules - heat maps of traits where the turquoise module is closely related to m6A score. **E.** Scatter plot showing the relationship between GS and MM in the turquoise module.

3.3 SMR analysis to identify PC-associated pathogenic genes

We performed SMR and HEIDI tests to identify proteins associated with PC. Among the 102 proteins that passed both tests (p_SMR < 0.05 and p_HEIDI > 0.05) in PC (supplement Table 2), three characteristic genes were found within the turquoise module containing 882 genes (Fig.3A): GCC2 (p_SMR=0.0094, p_HEIDI=0.4273), UBE2D3 (p_SMR=0.0187, p_HEIDI=0.7186), and

TMX1 (p_SMR=0.01238, p_HEIDI=0.0867). Furthermore, we plotted the SMR trajectories for GCC2, UBE2D3, and TMX1 (Figure 3B, C and D).

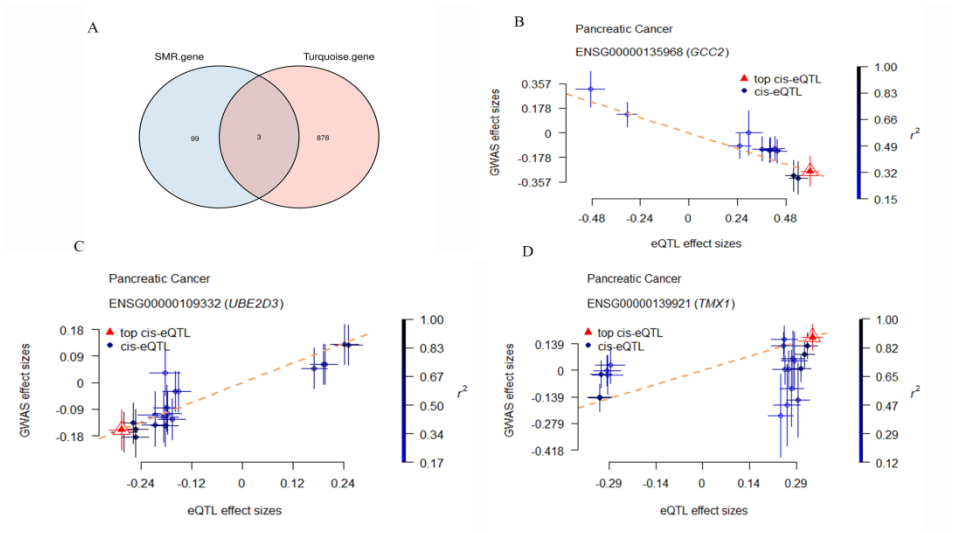

Figure 3 SMR analysis was performed to identify PC-related pathogenic genes. **A.** Venn diagram shows the intersection genes between the turquoise module and SMR. **B-D.** SMR trajectory plots for GCC2, UBEAD3, and TMX1, with orange dashed lines indicating estimated XY (xy) values at top cis-eQTLs (rather than regression lines) and error bars representing standard errors of SNP effects.

3.4 Performance evaluation and clinical pathological correlation of shared genetic signatures

Intersection analysis identified three pathogenic genes associated with PC, namely GCC2, UBEAD3, and TMX1. Validation using TCGA-PAAD samples demonstrated consistent differential expression of UBEAD3 (P=0.00373) and TMX1 (P= 1.36e-05), whereas the differential expression of GCC2 (P= 0.0543>0.05) was not statistically significant (Figure 4A, E, I). Upregulation of GCC2 and TMX1 and downregulation of UBE2D3 were observed in PC tissues. The prognostic evaluation was conducted through survival analysis (Figure 4B, F, J), with P-values for OS being 0.103 for GCC2, 0.057 for UBEAD3, and 0.001 for TMX1. ROC curves generated by the timeROC package revealed that only TMX1 had an AUC>0.6 among GCC2, UBEAD3, and TMX1 (Figure 4C, G, K). Diagnostic ROC curves were plotted (Figure 4D, H, and L). Further analysis of protein levels in PC tissues compared to normal pancreatic tissues using data from the HPA database showed consistency between IHC staining results for GCC2, UBEAD3, and TMX1 antibodies HPA035849, HPA003920 and HPA003085, respectively (Figure 5A, B, C). These findings validate previous observations at the transcriptional level, specifically regarding the association between high TMX1 expression and poor PC prognosis. Subsequently, statistical analysis was performed on TMX1 to determine its prognostic significance at a significance level of P<0.05. The clinical correlation analysis (Table l) revealed significant differences (P<0.05) in different N stages, overall stages, and grades between high and low expression of TMX1, suggesting a strong association between TMX1 and the clinicopathological features of PC.

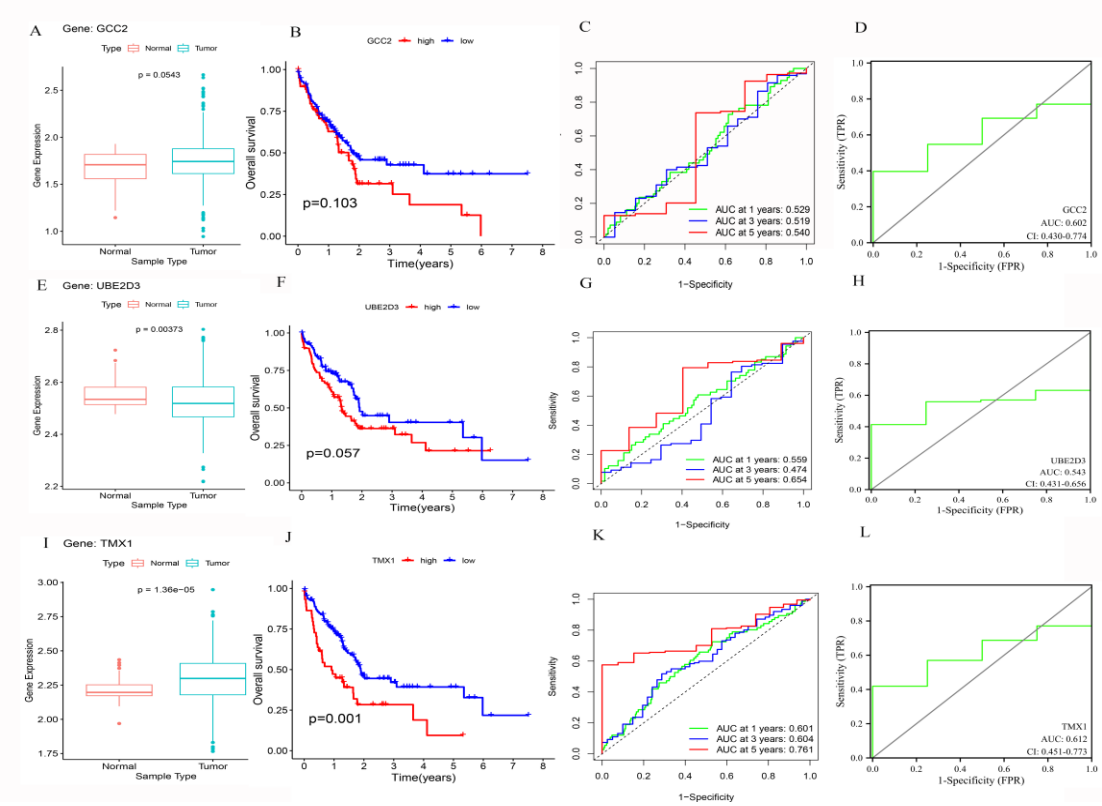

Figure 4 Performance evaluation of GCC2, UBEAD3, and TMX1. **A-D**. The differential box-plots (P=0.0543), survival curves (P=0.103), time-dependent ROC curves (1-year AUC=0.529, 3-year AUC=0.519, 5-year AUC=0.540), and diagnostic ROC curve (AUC=0.602) for GCC2 are shown. **E-H**.The differential box-plots (P=0.00373), survival curves (P=0.057>0.05), time-dependent ROC curves (1-year AUC = 0.559, 3-year AUC =0.474, 5-year AUC =0.554) and diagnostic ROC curve (AUC =0.543) for UBE2D3 are shown. **I-L.**The differential box-plots (P<1 .36e -05), survival curves (P=0.001), time-dependent ROC curves(1-yearAUC =0.601 , 3-yearAUC =0.604 , 5-yearAUC =0.761) and diagnostic ROC Curve (AUC =0.612) for TMX1 are shown.

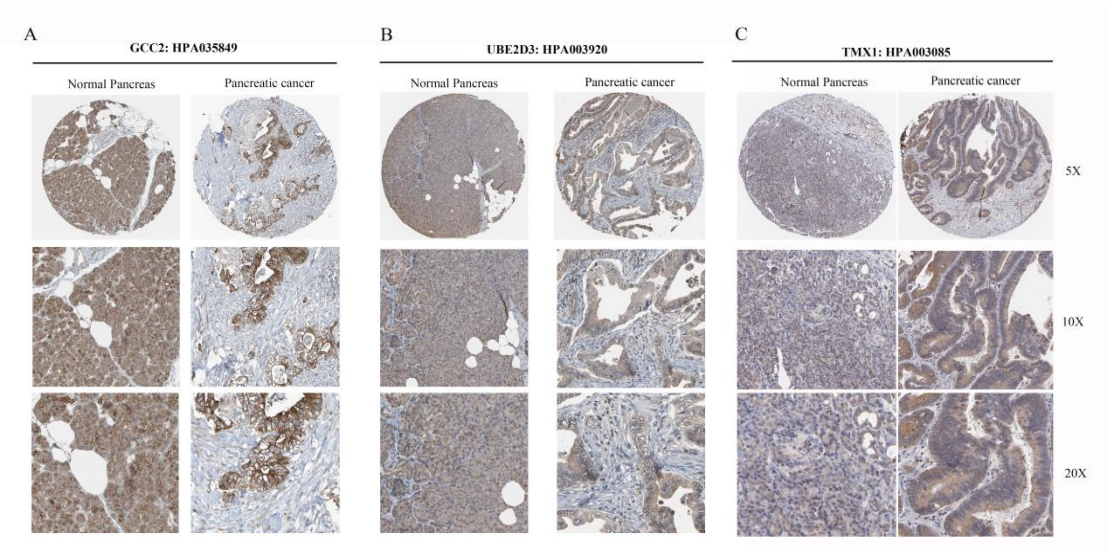

Figure 5 The expressions of GCC2, UBEAD3, and TMX1 proteins were confirmed. **A**. IHC staining revealed that the GCC2 protein had high expression levels in both normal pancreas tissues and PC tissues when using the

antibody HPA035849. **B**. IHC staining demonstrated that the UBE2D3 protein had low expression levels in both normal pancreas tissues and PC tissues when utilizing the antibody HPA003920. **C**. IHC staining indicated that the TMX1 protein had low expression levels in normal pancreas tissues but moderate expression levels in PC tissues when employing the antibody HPA003085. This finding was consistent with transcriptome-level results.

Table 1: Correlation between TMX1 and the clinicopathological features of PC

Characteristics	Low expression of TMX1	High expression of TMX1	P value
n	89	90	
Pathologic T stage, n (%)			0.052
T1&T2&T4	22 (12.4%)	12 (6.8%)	
T3	66 (37.3%)	77 (43.5%)	
Pathologic N stage, n (%)			0.015
N0	32 (18.4%)	18 (10.3%)	
N1	54 (31%)	70 (40.2%)	
Pathologic M stage, n (%)			0.764
M0	34 (40%)	46 (54.1%)	
M1	3 (3.5%)	2 (2.4%)	
Pathologic stage, n (%)			0.021
Stage I&Stage III&Stage IV	20 (11.4%)	9 (5.1%)	
Stage II	67 (38.1%)	80 (45.5%)	
Histologic grade, n (%)			0.023
G1	22 (12.4%)	9 (5.1%)	
G2	48 (27.1%)	48 (27.1%)	
G3	17 (9.6%)	31 (17.5%)	
G4	1 (0.6%)	1 (0.6%)	

3.5 PPI network analysis and GSEA enrichment analysis of the pathogenic gene of TMX1

GeneMANIA analysis revealed significant interactions between TMX1 and other genes (Figure 6A). Interestingly, we observed a close association between TMX1 and LRRK2, TXN (the thioredoxin), and TXNL1 in terms of their biological functions. Notably, the TXN system acts as an effector triggered by NADPH + H+/FAD oxidation-reduction reactions to maintain homeostasis, bioenergetics, detoxification drug networks, and cellular survival in oxidative stress-related diseases (Calandria et al., 2023). The primary function of TXNL1 is to regulate oxidative stress, thereby preserving cellular integrity by maintaining redox homeostasis. Additionally, TXNL1 exhibits a robust association with cancer therapeutics and diseases associated with oxidative stress (Zhao & Qi, 2021). Furthermore, our findings demonstrated that TMX1 and its associated genes primarily function in the regulation of ROS responses, including oxidative stress and hydrogen peroxide-induced cellular responses. Moreover, they played a negative modulatory role in these responses. Additionally, they are involved in controlling hydrogen peroxide-triggered cell death and oxidoreductase activity related to sulfur donors. To explore the potential biological functions of TMX1 in PC, we performed. The results revealed that reduced expression of TMX1 was predominantly associated with basal cell carcinoma occurrence, drug metabolism (particularly cytochrome P450 enzyme family), exogenous chemical metabolism, vitamin A metabolism, and ribosome synthesis and assembly (Figure 6B). Conversely, elevated expression of TMX1 primarily participates in crucial biological processes such as the regulation of immune response, control of cell cycle, cell communication, and maintenance of tissue structure (Figure 6C). Therefore, TMX1

may serve as a pivotal regulatory factor in PC and other diseases, and alterations in its expression levels can affect multiple biological pathways and disease progression.

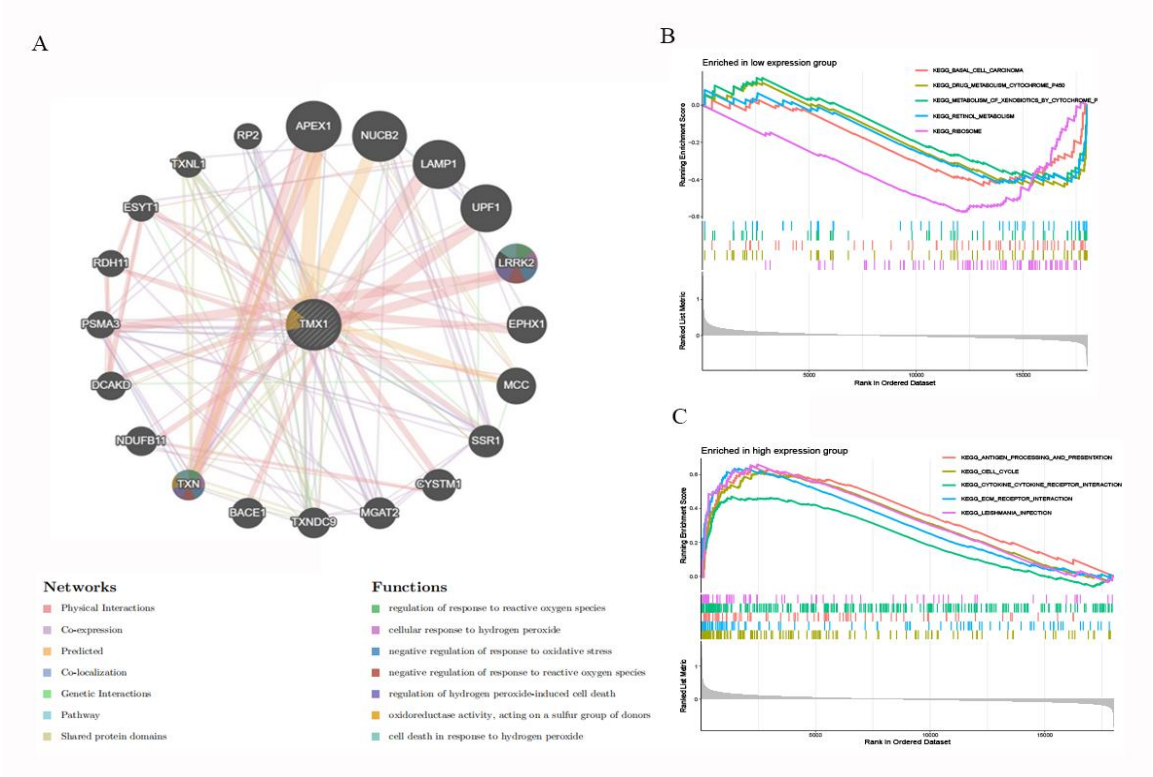

Figure 6 Biological processes associated with TMX1 and its related genes. **A**. The biological function of TMX1 and its related genes mainly involves regulating the response to reactive oxygen species. **B-C**. GSEA enrichment analysis was performed on the TMX1 high and low expression groups.

3.6 ScRNA-seq and stRNA-seq data analysis revealed the expression distribution of TMX1 in PC

To investigate the role of TMX1 in the TME at the single-cell transcriptome level, we analyzed the expression patterns of TMX1 across different cell types. Using t-SNE plots and bubble plots (Figures 7B and C), we visually annotated and examined the expression levels of TMX1 in various cell types. Monocytes exhibited the highest average expression level (close to 1), and a significant proportion of cells expressing this gene (over 60%), suggesting that TMX1 is predominantly active in monocytes and serves as a major contributor among these cell types. Initially, quality control was performed on the stRNA-seq data using the following filtering criteria: nFeature_Spatial_filt > 300 and nCount_Spatial_filt > 500 (Figure 7D). Subsequently, we plotted TMX1, TMX1+monocyte, TMX1-monocyte, and epithelial cells within PC tissue to identify overlapping regions at spatial capture locations (Figure 7E-H). Subsequently, we employed the mistyR algorithm (Tanevski et al., 2022) to facilitate spatial transcriptomic analysis of cell-cell interactions (Figure 7I-J).

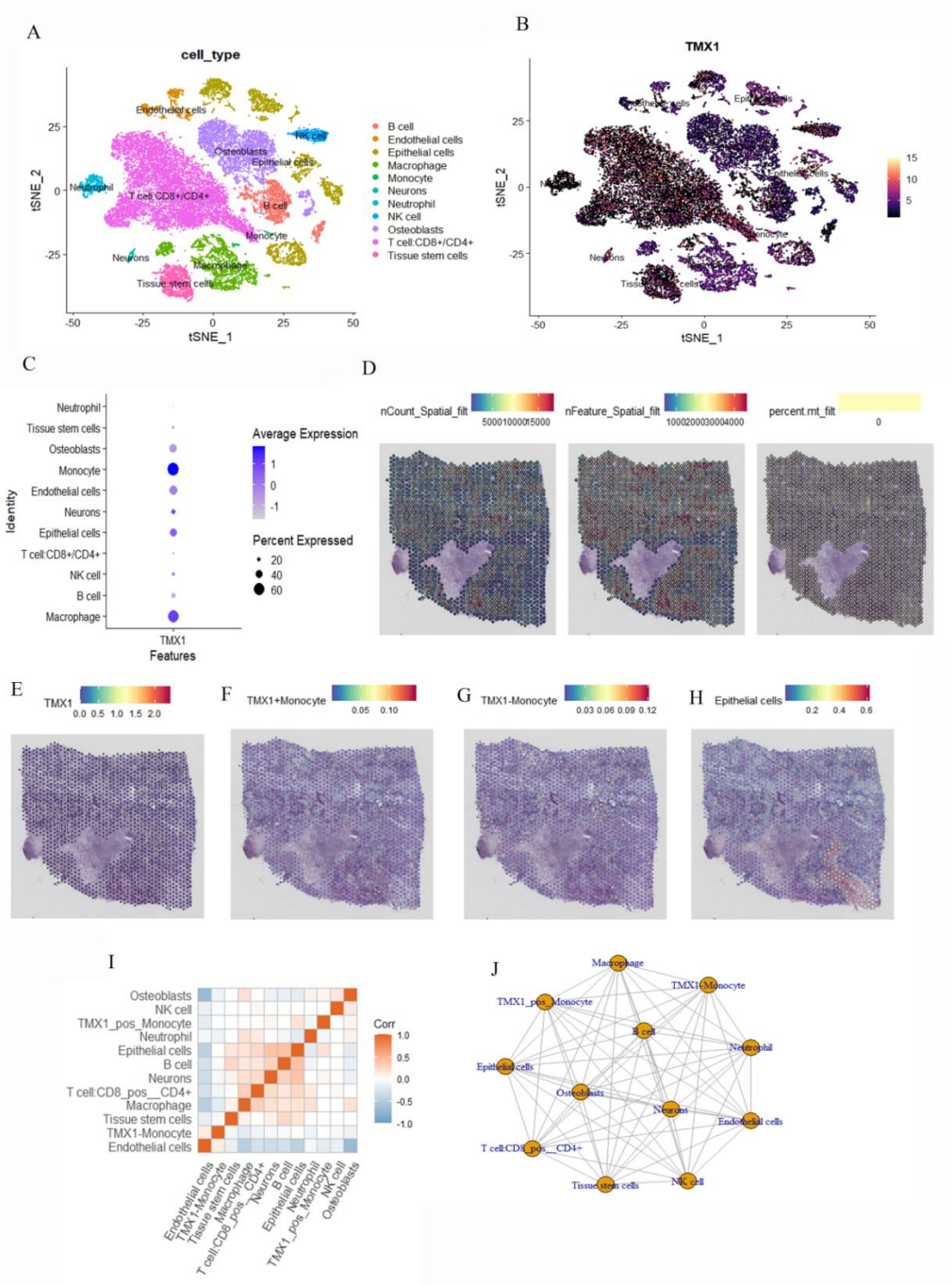

Figure 7 Data analysis of scRNA-seq and stRNA-seq. **A.** The utilization of t-SNE plot facilitates the reannotation of cells, thereby unveiling the cell types identified through marker genes. **B**. Feature maps expressed by TMX1. **C.**TMX1 expression bubble chart. **D.** Quality assurance of stRNA-seq data. **E-H.** Visualization of TMX1, TMX1+Monocyte, TMX1-Monocyte, and Epithelial cells in spatial transcriptome tissue sections of PC. **I.** Heat map depicting cell-cell interactions in spatial transcriptomics analysis. **J.** The spatial transcriptomic cell communication network diagram displays the weight and quantity of interactions between subsets of cells.

3.7 Immune Landscape Assessment

To investigate the immune landscape of patients with high and low TMX1 expression, we utilized the ssGSEA algorithm to analyze the abundance. Compared to patients with low TMX1 expression, those with high TMX1 expression exhibited augmented anti-tumor immune-related functions (Figure 8A), including central memory T cells (TCMs), Helper T cells, Eosinophils, Neutrophils, and Th2 cells. This observation suggests a positive correlation between high TMX1 expression and enhanced anti-tumor immunity. We employed the CIBERSORT algorithm to calculate the proportions of 22 immune cell subtypes in PC patients and considered a P-value threshold of <0.05, which was statistically significant (Figure 8B). Additionally, we employed the ssGSEA algorithm to investigate the association between TMX1 expression and immune cell subtype (Figure 8C). Our analysis revealed a positive correlation between TMX1 and Helper T cells, Th2 cells, TCMs, Neutrophils, Eosinophils, Th1 cells, Mast cells, Macrophages, and **Activated Dendritic Cells (**aDCs); however, a negative correlation was observed between CD56 bright NK cells, Th17cells, and Plasmacytoid dendritic cells (pDCs). To further elucidate these relationships, scatter plots were generated for selected cell types that met the criteria of a correlation coefficient R>0.3 (Figure 8D-F), including TCMs (P<0.001, R=0.357), Helper T cells (P<0.001, R=0.477), and Th2 cells (P<0.001, R=0.455). Immune correlation analysis supported these findings (Figure 8G), providing additional evidence of an association between TMX1 and m6A regulatory factors (Figure 8H).

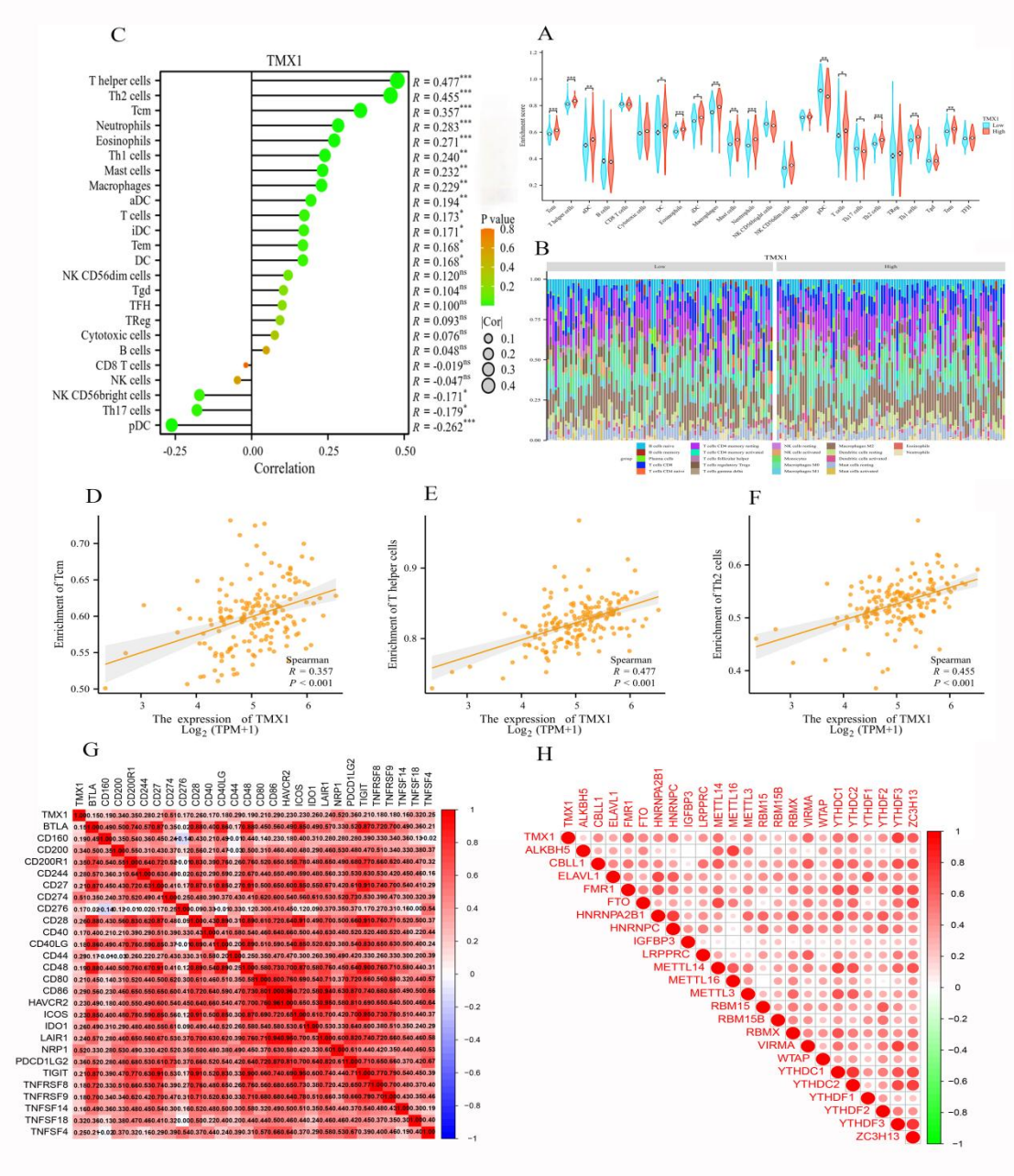

Figure 8 Immune landscape assessment. **A.** Differences in immune cell and immune function scores were observed between the high TMX1 group and the low TMX1 group. **B.** Relative proportions of immune cell infiltration were compared between the high TMX1 group and the low TMX1 group. **C.** The relationship between TMX1 expression in PC patients and subtypes of immune cells was investigated. **D-F.** Correlations between TMX1 expression and parameters were examined, including T Central Memory Cells, T Helper Cells, and Th2 Cells. **G.** A correlation heatmap was generated to illustrate the associations of TMX1 with immune-related genes. **H.** A bubble plot was used to visualize the correlation between TMX1 and m6A-related genes.

3.8 Drug Sensitivity Analysis

To anticipate the reaction to chemotherapy, we employed the pRRophetic algorithm to estimate chemotherapy response based on accessible half-maximal inhibitory concentration (IC_{50}) data from the Genomics of Drug Sensitivity in Cancer (GDSC) database for patients diagnosed with pancreatic adenocarcinoma (PAAD). Our investigation revealed that PAAD patients with decreased TMX1 expression demonstrated increased sensitivity to TAE684, Sunitinib, NPK76-II-72-1, GW843682X, Crizotinib, and AKT inhibitor VIII (P<0.001) (Figure 9A-F). Subsequently, we visualized the three-dimensional structures of these six small-molecule compounds using PubChem (Figure 9G-L). These findings emphasize the potential of drug sensitivity analysis to guide personalized treatment strategies and to establish a basis for precision therapy in patients with PC.

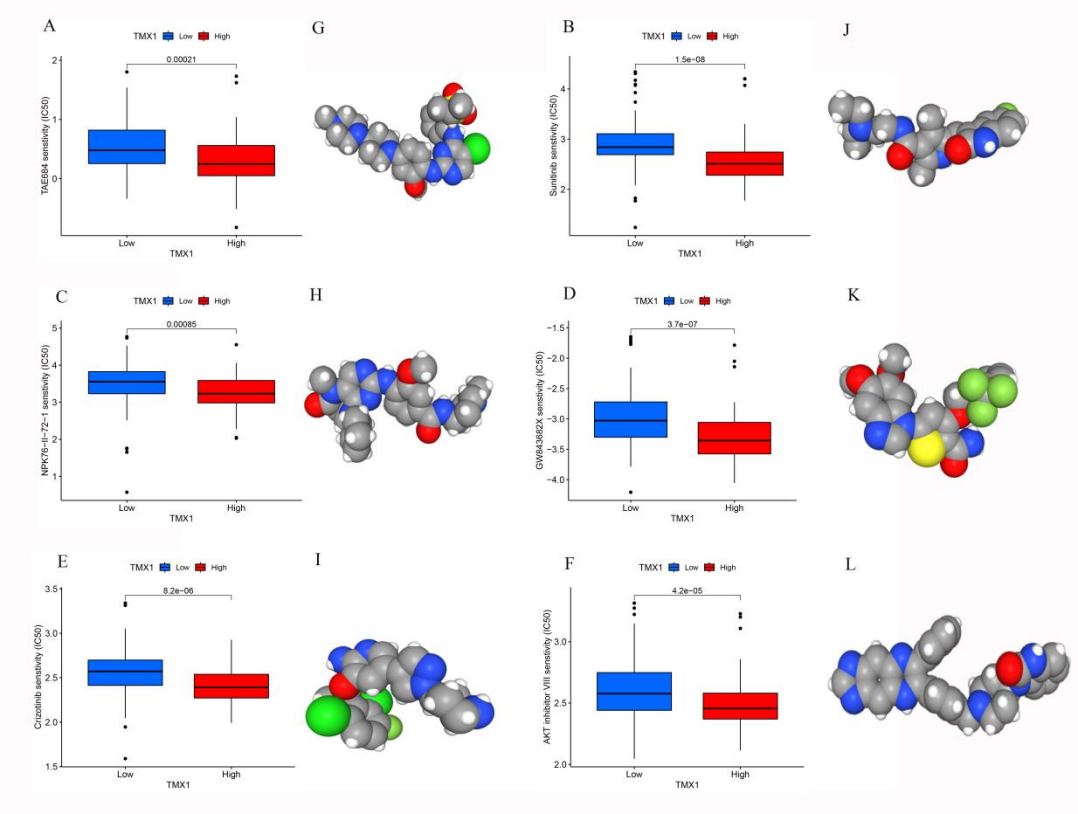

Figure 9 Drug sensitivity analysis in patients with PC. **A-F**. Comparison of drug sensitivity between patients classified into high TMX1 group and low TMX1 group. **G-L**. 3D structures corresponding to the aforementioned six drugs.

4 DISCUSSIONS

PC, especially pancreatic ductal adenocarcinoma, is a highly aggressive and drug-resistant nature of PC, coupled with its significant intratumoral heterogeneity and complex TME, which poses substantial challenges for diagnosis and treatment. Multi-omics approaches have emerged as widely utilized tools in cancer research to identify diagnostic or prognostic biomarkers and features, thereby enhancing our understanding of the fundamental genetics underlying pancreatic cancer (PC) (Cid-Arregui & Juarez, 2015).Furthermore, the advent of multiomics techniques has

significantly enhanced our understanding of the molecular mechanisms underlying diseases and has facilitated a paradigm shift in clinical treatment strategies (Golubnitschaja et al., 2016). M6A regulators have been implicated in oncogenic processes underlying cancer development (Liu et al., 2018).

The m6A modification process can be reversed by regulating m6A methyltransferases, demethylases, and binding proteins. Extensive research has established a significant correlation between m6A modification and cancer, wherein it facilitates self-renewal of tumor stem cells, enhances cancer cell growth and proliferation, and confers resistance to radiotherapy or chemotherapy (Mao et al., 2019). The collective body of evidence strongly indicates that m6A regulators have promising potential as targets for cancer therapy (McGuigan et al., 2018). The objective of this study was to investigate the effect of m6ARS on PC systematically.

In the upstream analysis, we screened for m6ARS at single-cell and global transcriptome levels based on AddModule scores, ssGSEA, and WGCNA analysis. Screening at the single-cell level accurately captures cell heterogeneity while considering the overall transcriptome level, which in turn reflects the overall characteristics of the TME. Simultaneously, we used the SMR method to integrate multi-omics data across different types of biological data to identify phenotypically related pathogenic genes, reduce the bias caused by confounders, and improve the reliability of causal inference. This series of multi-omics analyses led us to obtain three m6ARS, namely GCC2, UBE2D3, and TMX1.

To further investigate the clinical and pathological characteristics and prognosis of PC associated with the three m6ARS, we used TCGA-PAAD samples for validation purposes. The results indicated no significant difference in the expression levels of GCC2 (P=0.0543). Prognostic analysis revealed no statistical disparity between GCC2 and UBEAD3 in OS. Time-dependent ROC curve analysis and diagnostic ROC curve analysis yielded outcomes consistent with the survival analysis, indicating that neither GCC2 nor UBEAD3 possessed prognostic value. Only TMX1 exhibited concordance with the previously observed transcription levels based on the IHC staining results. Considering these findings, it is noteworthy that only TMX1 demonstrated differential prognostic significance, where high TMX1 expression was associated with poor prognosis in PC.

Gene-gene interaction analysis revealed a close association between TMX1 and its related genes, particularly LRRK2, TXN, and TXNL1. Notably, the TXN system functions as an NADPH + H+/FAD REDOX-triggered effector that plays a crucial role in maintaining homeostasis, bioenergetics, detoxification drug networks, and cell survival under conditions of oxidative stress-related diseases (Calandria et al., 2023). The primary role of TXNL1 lies in the regulation of oxidative stress and the maintenance of cellular integrity through REDOX homeostasis.Moreover, TXNL1 has significant implications for cancer treatment and the management of oxidative stress-related disorders (Zhao & Qi, 2021). Our findings demonstrate that TMX1 and its associated genes primarily participate in the regulation of reactive oxygen species responses, including oxidative stress, hydrogen peroxide-induced cellular response, negative modulation of these responses, and the control of cell death triggered by hydrogen peroxide and REDOX enzyme activity related to sulfur donors.Previous investigations have revealed that the TMX protein family comprises five membrane-bound tetratricopeptide repeat domain-containing proteins (TMX1, TMX2, TMX3, TMX4, and TMX5) (Oguro & Imaoka, 2019; Haugstetter et al., 2005; Sugiura et al., 2010; Kozlov et al., 2010; Matsuo et al., 2001). The proteins under consideration possess an N-terminal signaling sequence for targeting the endoplasmic reticulum (ER) and a functional thioredoxin (TRX)---like domain. Among the members of the TMX family, TMX1 has been extensively studied, exhibiting

a preference for interacting with membrane-binding folding capabilities and clients with folding defects (Pisoni et al., 2015). TMX1, which can form disulfide bonds in nascent proteins within the endoplasmic reticulum, is highly expressed on the mitochondria-associated membrane (MAM), where ER-mitochondrial Ca2+ flux occurs (Zhao et al., 2019). This flux plays a crucial role in regulating mitochondrial metabolism, which is often inhibited in tumor tissues, leading to chemotherapy resistance and increased tumor growth. As a sulfhydryl-based tumor suppressor, TMX1 enhances mitochondrial ATP production and apoptotic processes (Raturi et al., 2016). A previous analysis demonstrated TMX1 as an M6A-associated signature gene. According to previous studies, the relationship between m6A modification and oxidative stress is intricate. The interplay between oxidative stress and m6A modification and its significance in tumorigenesis and development is highly complex. M6A modification of genes associated with oxidative stress may regulate their own expression, thereby influencing the equilibrium between oxidation and antioxidation, as well as subsequent tumor occurrence and progression (Zhao et al., 2019; Sohrabi et al., 2019). Therefore, we speculate that TMX1 may contribute to tumor promotion, and the upregulation of TMX1 may affect the tumorigenesis of PC through oxidative stress, thus leading to the poor prognosis of PC.

The combination of spatial transcriptomics with scRNA-seq is a key component in linking pathological phenotypes of human tissues to molecular alterations, which defines knowledge of spatiotemporal molecular medicine and in situ intercellular molecular communication. Spatial transcriptomics provides high-throughput molecular profiles and location information via spatial barcode microarrays to achieve unbiased localization of transcripts across the entire tissue slice. Interestingly, in our single-cell analysis and spatial transcriptomics, we found that TMX1 is mainly expressed in monocytes. According to existing studies (Sohrabi et al., 2019), monocytes, regulated by oxidative stress, can affect the immune response and thus may be related to tumorigenesis and prognosis. These results support our finding that TMX1 may affect PC through oxidative stress.

Our research also revealed a significant correlation between TMX1 and immune infiltration in PC, which ultimately affects its prognosis. These findings suggest that future treatments for PC should adopt a comprehensive approach that combines aggressive therapy with immunotherapy (Finck et al., 2020). A combined approach that integrates immunotherapy with other modalities is regarded as a promising therapeutic strategy. Increasing evidence has demonstrated the pivotal role of T cells in immunotherapy (Winter et al., 2020). Specifically, we observed a significant positive correlation between TMX1 expression and the abundance of Helper T cells, Th2 cells, and TCMs. Ajina and Weiner (2020) previously reported the role of T helper cells in promoting the growth, invasion, and metastasis of PC cells. Jacenik et al. (2023) reported that Th2 cells play an important role in inhibiting the progression of colon cancer and PC. Goulart et al. (2021) elucidated the intricate interplay between T cells and various constituents of the tumor microenvironment (TME) in pancreatic cancer (PC) have been extensively studied (Duong et al., 2021).These findings suggest that TMX1 may serve as a predictive biomarker for PC prognosis and response to immunotherapy. In addition, our drug sensitivity analysis identified six potentially sensitive agents, including TAE684, Sunitinib, NPK76-II-72-1, GW843682X, Crizotinib, and AKT inhibitor VIII (Skaraite et al., 2023). Among them, sunitinib showed tha5 anticancer activity in the MIA PaCa-2 and PANC-1 cell lines. Crizotinib may be an effective drug for treating the peritoneal spread of PC by inhibiting cancer cell proliferation and invasion, at least in part by inhibiting HGF/MET signaling and RhoA activation (Takiguchi et al., 2017). NPK76-II-72-1, GW843682X, and AKT inhibitor VIII have not been studied in PC and may be potential PAAD

therapeutics, but further analysis is needed in the near future to provide new insights into the treatment of patients with PC (Skaraite et al., 2023).

However, our study had some limitations. First, this study relied on a public database, and there may have been sample selection bias. Second, although we validated m6ARS with PC progression and prognosis, the specific molecular mechanisms still require further experimental investigation. In addition, the role of m6ARS in the distant metastasis of PC has not been fully evaluated, and future studies should include more metastatic samples for verification.

5 CONCLUSIONS

This study, which identified m6ARS through a combination of single-cell sequencing and SMR analysis, revealed the multilayered role of m6ARS in PC, including its influence on the TIME, the value of prognostic assessment, and the regulation of therapeutic response. Notably, we developed an effective prognostic profile based on TMX1-related genes in PC. TMX1 may become a powerful predictive biomarker of cancer prognosis and immunotherapy response in PC, and targeting TMX1 to mediate oxidative stress may be a novel therapeutic approach for PC, providing a new target for future drug development.

References

Ajina, R., & Weiner, L. M. (2020). T-Cell Immunity in Pancreatic Cancer. Pancreas, 49(8), 1014–1023.

Ansari, D., Gustafsson, A., & Andersson, R. (2015). Update on the management of pancreatic cancer: surgery is not enough. World journal of gastroenterology, 21(11), 3157–3165.

Burgess, S., Timpson, N. J., Ebrahim, S., & Davey Smith, G. (2015). Mendelian randomization: where are we now and where are we going?. International journal of epidemiology, 44(2), 379–388.

Calandria, J. M., Bhattacharjee, S., Kala-Bhattacharjee, S., Mukherjee, P. K., Feng, Y., Vowinckel, J., Treiber, T., & Bazan, N. G. (2023). Elovanoid-N34 modulates TXNRD1 key in protection against oxidative stress-related diseases. Cell death & disease, 14(12), 819.

Cid-Arregui, A., & Juarez, V. (2015). Perspectives in the treatment of pancreatic adenocarcinoma. World journal of gastroenterology, 21(31), 9297–9316.

Davey Smith, G., & Hemani, G. (2014). Mendelian randomization: genetic anchors for causal inference in epidemiological studies. Human molecular genetics, 23(R1), R89–R98.

Digre, A., & Lindskog, C. (2021). The Human Protein Atlas-Spatial localization of the human proteome in health and disease. Protein science: a publication of the Protein Society, 30(1), 218–233.

Duong, H. Q., Than, V. T., Nguyen, H. T., Nguyen, P. T., Thi, H. T. H., Bui, T. N. H., Dang, V. P. L., Dinh, T. T., You, K. S., Dang, T. H., & Seong, Y. S. (2021). Anaplastic lymphoma kinase inhibitor NVP TAE684 suppresses the proliferation of human pancreatic adenocarcinoma cells. Oncology reports, 45(4), 28.

Finck, A., Gill, S. I., & June, C. H. (2020). Cancer immunotherapy comes of age and looks for maturity. Nature communications, 11(1), 3325.

Fu, Y., & Zhuang, X. (2020). m6A-binding YTHDF proteins promote stress granule formation. Nature chemical biology, 16(9), 955–963.

Golubnitschaja, O., Baban, B., Boniolo, G., Wang, W., Bubnov, R., Kapalla, M., Krapfenbauer, K., Mozaffari, M. S., & Costigliola, V. (2016). Medicine in the early twenty-first century: paradigm and anticipation - EPMA position paper 2016. The EPMA journal, 7(1), 23.

Goulart, M. R., Stasinos, K., Fincham, R. E. A., Delvecchio, F. R., & Kocher, H. M. (2021). T cells in pancreatic cancer stroma. World journal of gastroenterology, 27(46), 7956–7968.

Hänzelmann, S., Castelo, R., & Guinney, J. (2013). GSVA: gene set variation analysis for microarray and RNA-seq data. BMC bioinformatics, 14, 7.

Haugstetter, J., Blicher, T., & Ellgaard, L. (2005). Identification and characterization of a novel thioredoxin-related transmembrane protein of the endoplasmic reticulum. The Journal of biological chemistry, 280(9), 8371–8380.

He, L., Li, H., Wu, A., Peng, Y., Shu, G., & Yin, G. (2019). Functions of N6-methyladenosine and its role in cancer. Molecular cancer, 18(1), 176.

Hou, G., Zhao, X., Li, L., Yang, Q., Liu, X., Huang, C., Lu, R., Chen, R., Wang, Y., Jiang, B., & Yu, J. (2021). SUMOylation of YTHDF2 promotes mRNA degradation and cancer progression by increasing its binding affinity with m6A-modified mRNAs. Nucleic acids research, 49(5), 2859–2877.

Hou, J., Wang, Z., Li, H., Zhang, H., & Luo, L. (2020). Gene Signature and Identification of Clinical Trait-Related m6 A Regulators in Pancreatic Cancer. Frontiers in genetics, 11, 522.

Jacenik, D., Karagiannidis, I., & Beswick, E. J. (2023). Th2 cells inhibit growth of colon and pancreas cancers by promoting anti-tumorigenic responses from macrophages and eosinophils. British journal of cancer, 128(2), 387–397.

Joly, J. H., Lowry, W. E., & Graham, N. A. (2021). Differential Gene Set Enrichment Analysis: a statistical approach to quantify the relative enrichment of two gene sets. Bioinformatics (Oxford, England), 36(21), 5247–5254.

Kozlov, G., Määttänen, P., Thomas, D. Y., & Gehring, K. (2010). A structural overview of the PDI family of proteins. The FEBS journal, 277(19), 3924–3936.

Langfelder, P., & Horvath, S. (2008). WGCNA: an R package for weighted correlation network analysis. BMC bioinformatics, 9, 559.

Liu, Z. X., Li, L. M., Sun, H. L., & Liu, S. M. (2018). Link Between m6A Modification and Cancers. Frontiers in bioengineering and biotechnology, 6, 89.

Mao, Y., Dong, L., Liu, X. M., Guo, J., Ma, H., Shen, B., & Qian, S. B. (2019). m6A in mRNA coding regions promotes translation via the RNA helicase-containing YTHDC2. Nature communications, 10(1), 5332.

Matsuo, Y., Akiyama, N., Nakamura, H., Yodoi, J., Noda, M., & Kizaka-Kondoh, S. (2001). Identification of a novel thioredoxin-related transmembrane protein. The Journal of biological chemistry, 276(13), 10032–10038.

McGuigan, A., Kelly, P., Turkington, R. C., Jones, C., Coleman, H. G., & McCain, R. S. (2018). Pancreatic cancer: A review of clinical diagnosis, epidemiology, treatment and outcomes. World journal of gastroenterology, 24(43), 4846–4861.

Oerum, S., Meynier, V., Catala, M., & Tisné, C. (2021). A comprehensive review of m6A/m6Am RNA methyltransferase structures. Nucleic acids research, 49(13), 7239–7255.

Oguro, A., & Imaoka, S. (2019). Thioredoxin-related transmembrane protein 2 (TMX2) regulates the Ran protein gradient and importin-β-dependent nuclear cargo transport. Scientific reports, 9(1), 15296.

Pisoni, G. B., Ruddock, L. W., Bulleid, N., & Molinari, M. (2015). Division of labor among oxidoreductases: TMX1 preferentially acts on transmembrane polypeptides. Molecular biology of the cell, 26(19), 3390–3400.

Raturi, A., Gutiérrez, T., Ortiz-Sandoval, C., Ruangkittisakul, A., Herrera-Cruz, M. S., Rockley, J. P., Gesson, K., Ourdev, D., Lou, P. H., Lucchinetti, E., Tahbaz, N., Zaugg, M., Baksh, S., Ballanyi, K., & Simmen, T. (2016). TMX1 determines cancer cell metabolism as a thiol-based modulator of ER-mitochondria Ca2+ flux. The Journal of cell biology, 214(4), 433–444.

Skaraite, I., Maccioni, E., & Petrikaitė, V. (2023). Anticancer Activity of Sunitinib Analogues in Human Pancreatic Cancer Cell Cultures under Normoxia and Hypoxia. International journal of molecular sciences, 24(6), 5422.

Sohrabi, Y., Lagache, S. M. M., Schnack, L., Godfrey, R., Kahles, F., Bruemmer, D., Waltenberger, J., & Findeisen, H. M. (2019). mTOR-Dependent Oxidative Stress Regulates oxLDL-Induced Trained Innate Immunity in Human Monocytes. Frontiers in immunology, 9, 3155.

Stuart, T., Butler, A., Hoffman, P., Hafemeister, C., Papalexi, E., Mauck, W. M., 3rd, Hao, Y., Stoeckius, M., Smibert, P., & Satija, R. (2019). Comprehensive Integration of Single-Cell Data. Cell, 177(7), 1888–1902.e21.

Sugiura, Y., Araki, K., Iemura, S., Natsume, T., Hoseki, J., & Nagata, K. (2010). Novel thioredoxin-related transmembrane protein TMX4 has reductase activity. The Journal of biological chemistry, 285(10), 7135–7142.

Sung, H., Ferlay, J., Siegel, R. L., Laversanne, M., Soerjomataram, I., Jemal, A., & Bray, F. (2021). Global Cancer Statistics 2020: GLOBOCAN Estimates of Incidence and Mortality Worldwide for 36 Cancers in 185 Countries. CA: a cancer journal for clinicians, 71(3), 209–249.

Taketo, K., Konno, M., Asai, A., Koseki, J., Toratani, M., Satoh, T., Doki, Y., Mori, M., Ishii, H., & Ogawa, K. (2018). The epitranscriptome m6A writer METTL3 promotes chemo- and radioresistance in pancreatic cancer cells. International journal of oncology, 52(2), 621–629.

Takiguchi, S., Inoue, K., Matsusue, K., Furukawa, M., Teramoto, N., & Iguchi, H. (2017). Crizotinib, a MET inhibitor, prevents peritoneal dissemination in pancreatic cancer. International journal of oncology, 51(1), 184–192.

Tanevski, J., Flores, R. O. R., Gabor, A., Schapiro, D., & Saez-Rodriguez, J. (2022). Explainable multiview framework for dissecting spatial relationships from highly multiplexed data. Genome biology, 23(1), 97.

Thanassoulis, G., & O'Donnell, C. J. (2009). Mendelian randomization: nature's randomized trial in the post-genome era. JAMA, 301(22), 2386–2388.

Wang, J., Ishfaq, M., Xu, L., Xia, C., Chen, C., & Li, J. (2019). METTL3/m6A/miRNA-873-5p Attenuated Oxidative Stress and Apoptosis in Colistin-Induced Kidney Injury by Modulating Keap1/Nrf2 Pathway. Frontiers in pharmacology, 10, 517.

Winter, H., van den Engel, N. K., Rüttinger, D., Schmidt, J., Schiller, M., Poehlein, C. H., Löhe, F., Fox, B. A., Jauch, K. W., Hatz, R. A., & Hu, H. M. (2007). Therapeutic T cells induce tumor-directed chemotaxis of innate immune cells through tumor-specific secretion of chemokines and stimulation of B16BL6 melanoma to secrete chemokines. Journal of translational medicine, 5, 56.

Wolfgang, C. L., Herman, J. M., Laheru, D. A., Klein, A. P., Erdek, M. A., Fishman, E. K., & Hruban, R. H. (2013). Recent progress in pancreatic cancer. CA: a cancer journal for clinicians, 63(5), 318–348.

Xiao, B., Liu, L., Li, A., Xiang, C., Wang, P., Li, H., & Xiao, T. (2020). Identification and Verification of Immune-Related Gene Prognostic Signature Based on ssGSEA for Osteosarcoma. Frontiers in oncology, 10, 607622.

Yang, H., Liu, D., Zhao, C., Feng, B., Lu, W., Yang, X., Xu, M., Zhou, W., Jing, H., & Yang, J. (2021). Mendelian randomization integrating GWAS and eQTL data revealed genes pleiotropically associated with major depressive disorder. Translational psychiatry, 11(1), 225.

Zhan, Z. Q., & Li, J. X. (2024). Dissecting the roles of oxidative stress gene expression in atopic dermatitis. Journal of the European Academy of Dermatology and Venereology: JEADV, 38(10), e914–e916.

Zhao, J. M., & Qi, T. G. (2021). The role of TXNL1 in disease: treatment strategies for cancer and diseases with oxidative stress. Molecular biology reports, 48(3), 2929–2934.

Zhao, Z., Wu, Y., Zhou, J., Chen, F., Yang, A., & Essex, D. W. (2019). The transmembrane protein disulfide isomerase TMX1 negatively regulates platelet responses. Blood, 133(3), 246–251.

Zhu, Z., Zhang, F., Hu, H., Bakshi, A., Robinson, M. R., Powell, J. E., Montgomery, G. W., Goddard, M. E., Wray, N. R., Visscher, P. M., & Yang, J. (2016). Integration of summary data from GWAS and eQTL studies predicts complex trait gene targets. Nature genetics, 48(5), 481–487.